Imaging of Cyclotron Emission from Edge Channels in Quantum Hall Conductors

K. Ikushima, H. Sakuma, and S. Komiyama
Department of Basic Science, University of Tokyo, Komaba, Meguro-ku, Tokyo 153-8902, Japan

K. Hirakawa
Institute of Industrial Science, University of Tokyo, Komaba, Meguro-ku, Tokyo 153-8505, Japan
(Received 1 April 2004; published 29 September 2004)

A local probing technique of cyclotron emission is applied to image nonequilibrium electrons generated along edge channels in quantum Hall conductors. In a lower-magnetic field region of a quantum Hall state plateau (filling factor $2 < \nu$), cyclotron emission is found to occur along the boundary of a conductor on the side of lower potential (with positive Hall voltage). The emission indicates that electrons are accumulated in the first-excited Landau level, while they are depleted in the lowest Landau level along the boundary as a consequence of adiabatic-transport.

DOI: 10.1103/PhysRevLett.93.146804 PACS numbers: 73.43.Qt, 07.60.Pb, 73.43.Fj, 78.66.–w

In finite two-dimensional electron gas (2DEG) layers at strong magnetic fields, Landau level (LL) energies increase to cross the Fermi level at their boundaries, forming current-carrying one-dimensional edge channels. In the regime of the quantum Hall effect (QHE), the edge channels play substantial roles, giving rise to a number of remarkable effects such as the occurrence of anomalous longitudinal or Hall resistance [1,2], the suppression of Schunikov–de Haas oscillations, and the occurrence of nonlocal resistance [3–8]. All these effects are brought about by a common physical feature, the absence of local equilibrium. That is, scattering between different edge channels (or between one edge channel and a bulk state) at the same boundary is strongly suppressed, so that they can be occupied with electrons up to different energies. The characteristic features of such adiabatic transport are evident and well established through extensive studies of resistance measurements at small currents (below 1 μA). At larger currents, however, adiabatic features diminish [9,10] and the edge-channel nonequilibrium is less understood. It may be of definite importance to directly visualize those nonequilibrium electrons in order to achieve a better understanding at larger currents. Merz *et al.* [11] found a sharp photoresponse in resistance, occurring when the edge region was locally excited via cyclotron resonance (CR). Similar edge photovoltage measurements suggested nonparabolicity in the edge confinement potential [12]. Unfortunately, these studies do not directly probe nonequilibrium electrons generated in the adiabatic transport, because resistance change induced by CR excitation was studied. Several techniques of scanning microscopes have been developed for probing QHE conductors [13,14]. However, these techniques are limited for studying either equilibrium properties [13] or electrostatic-potential profiles [14].

Local probing of cyclotron emission (CE) has recently proven to be a powerful tool to study nonequilibrium electrons [15,16]. The significant advantage over preceding studies [11,12] is that (i) the CE is obtained without external excitation and (ii) it provides a direct measure of the local density profile of excess electrons (holes) in LLs. Earlier studies have revealed generation of nonequilibrium electrons (holes) at the current-entry (exit) corner of Hall bars, called the "hot spots" [15]. They also visualized spatial evolution of the current-induced QHE breakdown [16]. Up to the present time, however, edge channels populated in a nonequilibrium fashion have not been tackled because the expected CE intensity is below the sensitivity limit of the available optical system.

Figure 1(a) illustrates a scanning-type THz microscope developed for the present study [17]. Both the sensitivity (a few fWs over 1 sec integration time) and the resolution (50 μm) have been significantly improved compared to the earlier systems [15,16]. Cyclotron radiation emitted from a point of a 2DEG layer is collected by a silicon solid immersion lens (SIL) and refocused onto a highly sensitive QHE detector [18] by a condenser lens. By moving the Hall bar by a mechanical *XY* stage, the focal point of the SIL scans the 2DEG layer. The QHE detector, fabricated on a GaAs/AlGaAs single heterostructure crystal with an electron density n_s of 2.7×10^{15} m^{-2} and a mobility of μ of 100 m^2/V s yields a narrow-

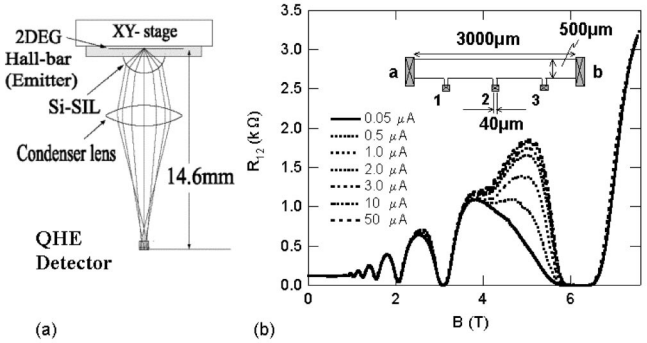

FIG. 1. (a) Schematic of the applied THz microscope and (b) Shubnikov–de Haas oscillations for the currents I_{ab} from 0.05 through 50 μA. The inset shows the Hall bar sample.

band photoresponse (with a relative bandwidth of 2%) at the cyclotron resonance frequency with a sensitivity of noise equivalent power, NEP $\sim 10^{-15}$ W/Hz$^{1/2}$.

In this work, we find weak CE in a narrow strip region along one boundary of Hall bars. The boundary is on the lower-potential side (with positive Hall voltage), while no CE is seen on the opposite boundary. The CE is visible only on the lower-magnetic field side of a QHE plateau (filling factor, $2 < \nu$), where Shubnikov–de Haas oscillations are significantly suppressed at small currents: The CE, however, emerges at larger currents (10–150 μA), where the adiabatic transport features have been less evident in resistance measurements. The findings suggest that (i) the nonequilibrium electron distribution, originally in an edge channel, develops to extend into the boundary of bulk state at larger currents, introducing electron accumulation in the higher LL and depletion in the lower LL at the boundary and (ii) this anomalous distribution makes the inter-LL direct radiative transition of electrons possible. The apparent smearing of adiabatic-transport features is consistent with the expectation that the amplitude of nonequilibrium population is limited by the LL energy spacing.

Samples are 3-mm-long and 0.5-mm-wide Hall bars fabricated via the conventional lithography method in a GaAs/AlGaAs heterostructure crystal with $n_s = 3.0 \times 10^{15}$ m^{-2} and $\mu = 30$ m^2/V s [inset of Fig. 1(b)]. All the measurements are made at $T = 4.2$ K. As shown in Fig. 1(b), Shubnikov–de Haas oscillations at low currents ($I_{ab} < 1$ μA) are significantly suppressed on the lower-magnetic-field side of the $\nu = 2$ QHE plateau ($B = 6.1$ T) due to decoupling between edge and bulk states [4–6]. As is well known, the longitudinal resistance R_{12} starts increasing as the current I_{ab} increases since the inter-edge-bulk scattering is promoted. The increase of resistance is saturated for $I_{ab} > 2$ μA, which has been suggested to be due to a saturation of the amplitude of nonequilibrium population at about $\hbar\omega_c$ [9,10,19].

To study CE, we record the modulation signal of the detector in the microscope [Fig. 1(a)], where I_{ab} is modulated between zero and a given amplitude (30 Hz). While the microscope is placed in a superconducting solenoid, the magnetic fields for the sample and the detector, B and B_D, can be chosen independently by finely adjusting the microscope position with respect to the solenoid center. Figure 2 displays CE images obtained at $I_{ab} = 50$ μA for different filling factors, where $B \approx B_D \approx 6.0$ T (the wavelengths of detected radiation centered at $\lambda = 123.3$ μm) [20]. In the QHE plateau at $\nu = 2.0$ [Fig. 2(b)] and in a transition region of $\nu < 2$ [Fig. 2(c)], no CE is seen except at the two hot spots [15,16]. Novel CE is found along the lower boundary at $\nu = 2.22$ [Fig. 2(a)], where the first-excited orbital LL is lightly occupied with electrons. As seen in Fig. 3, the region of CE is as narrow as the resolution limit of the microscope (50 μm). Additional measurements confirmed that the profile of CE is unchanged up to $I_{ab} = 150$ μA. The inset of Fig. 3 shows that the longitudinal voltage, V_{12}, is nearly proportional to I_{ab}, and the intensity of CE, studied at the maximum point of $Y = 860$ μm in Fig. 3, increases in proportion to the electrical input power dissipated in the Hall bar, $V_{12}I_{ab} \propto I_{ab}^2$, over the range $I_{ab} < 150$ μA.

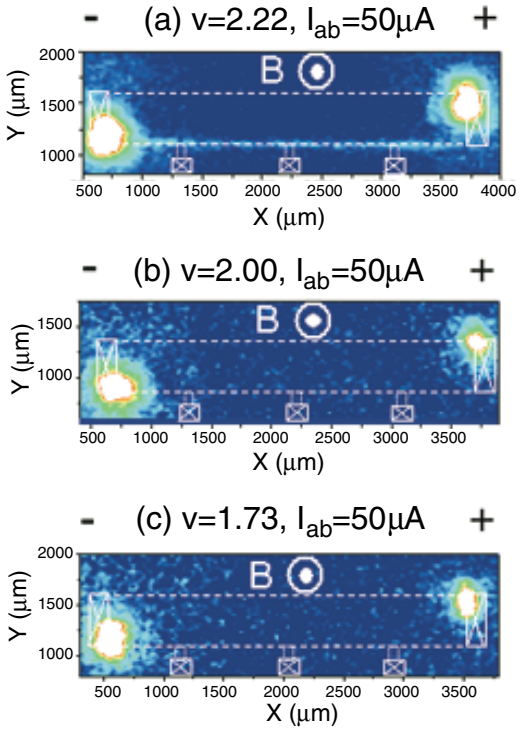

FIG. 2 (color). CE images at $I_{ab} = 50$ μA for $\nu = 2.22$ (a), $\nu = 2.00$ (b), and $\nu = 1.73$ (c). The white broken lines mark the boundary of the Hall bar (3 mm × 0.5 mm).

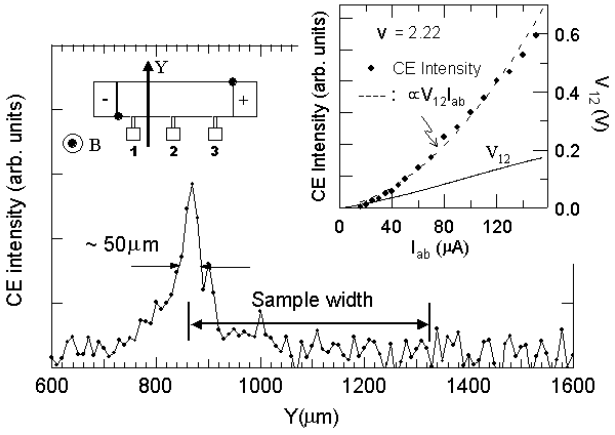

FIG. 3. Cross-sectional profile of the CE along the Y axis at $X = 1710$ μm. The inset shows the CE intensity and the longitudinal voltage V_{12} against I_{ab}.

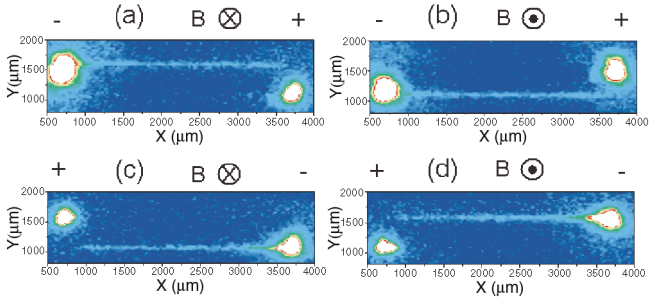

FIG. 4 (color). CE images obtained in four different polarities of the magnetic field and the current: (a) $(-B, I_{ab})$, (b) (B, I_{ab}), (c) $(-B, -I_{ab})$, and (d) $(B, -I_{ab})$.

The CE systematically alternates its location between opposite boundaries upon the reversal of the polarities of B and I_{ab}, as demonstrated in Fig. 4. This assures that the CE found here is free from device-specific asymmetry and is of an intrinsic origin. The boundary of CE is on the side of the lower potential for electrons (with positive Hall voltage) [21]. Figures 2(a) and 4(a)–4(d), along with additional measurements not shown here, suggest that the intensity of CE is nearly constant along the boundary (X axis) [22].

The CE intensity integrated along the boundary ($I_{ab} = 50\ \mu$A) is displayed against ν with closed circles in Fig. 5 [20], where the existence of CE for $2.1 < \nu$ and the absence for $\nu < 1.9$ are confirmed. It is to be noted that on either side of the QHE plateau the electron system is equally dissipative with comparable magnitudes of R_{12}.

To study spectrum, the CE intensity at the point of $Y = 860\ \mu$m in Fig. 3 is studied as a function of B, where B_D is fixed at 5.934 T ($\lambda = 124.6\ \mu$m). The inset of Fig. 5 displays the obtained resonant spectrum, which proves that the emission does arise from the inter-LL transition [23].

We now wish to interpret the findings of this work. The CE is seen only in the condition $2 < \nu$, where partially occupied, dissipative $n = 1$ LL coexists with fully occupied, dissipationless $n = 0$ LL. Since the two LLs are practically decoupled at low currents, the electrochemical potentials of the $n = 0$ LL, μ_0 (μ_0'), and those of the $n = 1$ LL, μ_1 (μ_1') take on different values on the respective boundaries (Fig. 6) [5,6,8,9]. As a general feature, we can assume $\mu_0 - \mu_1 > 0$ and $\mu_1' - \mu_0' > 0$, so that the Joule heating should be minimized. The difference, $\mu_0 - \mu_1$ or $\mu_1' - \mu_0'$, increases as I_{ab} increases. As shown in Fig. 6, when $\mu_1' - \mu_0'$ reaches $\hbar\omega_c$, μ_0' must enter the bulk region. This implies that the depletion region in the $n = 0$ LL extends into the bulk states. Since the electrostatic potential as well as the LL energies are thereby lowered, excess electrons are introduced into the upper $n = 1$ LL to nearly compensate the depletion in the lower $n = 0$ LL [9]. Thus, the local nonequilibrium population at the lower-potential boundary must be accompanied by depletion in the lower $n = 0$ LL and accumulation in the upper $n = 1$ LL. We interpret that this anomalous population gives rise to the observed inter-LL radiative transition (CE) as indicated by the thick arrow in Fig. 6. The model in the above also accounts for the earlier suggested saturation of $\mu_1' - \mu_0'$ at about $\hbar\omega_c$ [9,10,19].

At the higher-potential boundary (region "A" in Fig. 6) where $\mu_0 - \mu_1 > 0$, excess electrons in the $n = 0$ edge channel will tunnel to the $n = 1$ edge channel. After having tunneled, the electrons will rapidly fall into the bulk region releasing their excess energies to the lattice, probably via acoustical phonon emission. At this boundary, however, CE does not occur because there are no available holes. The nonequilibrium electrons entering the bulk region, in turn, traverse the interior region [24], "B," until they reach the opposite lower-potential boundary (region "C"), where they are accumulated in the $n = 1$ LL. They, in turn, exert transition to the $n = 0$ LL either via CE as discussed in the above, or via a nonradiative transition process (elastic tunneling to the

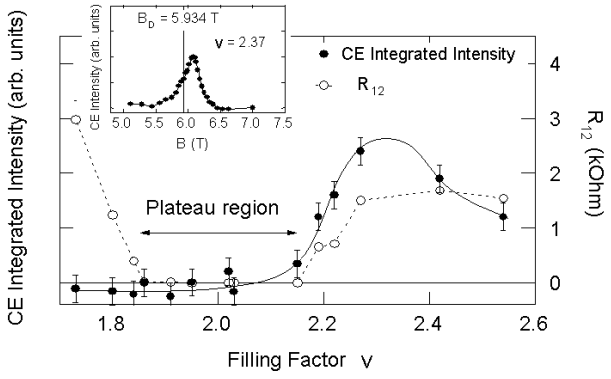

FIG. 5. The CE intensity integrated along the sample boundary and the longitudinal resistance R_{12}, against ν. The inset shows the CE spectrum.

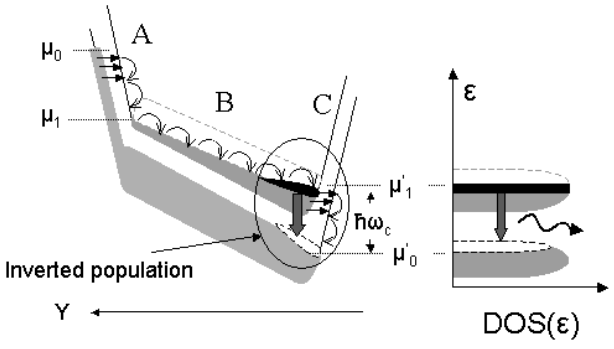

FIG. 6. Schematic representation of the energy profile of two Landau levels (on the left), and the density of states along with electron population (on the right), in the case when $\mu_1' - \mu_0' > \hbar\omega_c$.

$n = 0$ edge states followed by energy relaxation as marked by smaller arrows in Fig. 6).

The threshold current I_c, at which $\mu_1' - \mu_0'$ reaches $\hbar\omega_c$, is roughly estimated to be $I_c = 2$–3 μA from the relation $(\mu_S - \mu_D)/\{1 + (\rho_{xy}/\rho_{xx})(W/L)\} = \hbar\omega_c$ (μ_S and μ_D: the electrochemical potentials of the source and the drain contacts), where ρ_{xy} and ρ_{xx} are, respecetively, the Hall and the longitudinal resistivities of the $n = 1$ LL, and L and W are the length and the width of the Hall bar ($\rho_{xy}/\rho_{xx} = 10$–20 and $W/L = 1/6$ in the present conductor) [9]. Unfortunately, I_c was not identified in the experiments because the CE became invisible for $I_{ab} < 10$ μA due to the sensitivity limit of our microscope.

The integrated power of CE from the boundary (except the hot spot) is roughly estimated to be on the order of 1 pW at $I_{ab} = 50$ μA, corresponding to a luminous efficiency of 6×10^{-8} ($V_{xx} \times I_{ab} = 16.5$ μW). The small efficiency may reflect the fact that (i) most of the excess energies of nonequilibrium electrons is released to the lattice during the drift motion in the interior region B and (ii) the nonradiative process dominates in region C.

Letting f_n be the occupation probability of the nth LL, the existence of CE is a proof that $f_1/f_0 > (\nu - 2)/2$, where $f_0 = 1$ and $f_1 = (\nu - 2)/2$ in the equilibrium state. Since f_1/f_0 is made larger as the rate of nonradiative transition is suppressed, population inversion, $f_1/f_0 > 1$, may be expected if the rate of edge-state tunnel transition ($n = 1 \rightarrow 0$) is below a certain threshold. Although it is difficult to quantify, negative biasing of a side gate may help suppressing the tunnel rate. The QHE edge channels might thus be viewed as a potential system for THz wave amplification. We should also mention that lasing was earlier proposed on the basis of population inversion of LLs in appropriately designed QHE devices [25].

In summary, we have applied a highly sensitive scanning THz microscope for studying unequally populated edge channels. CE is found to occur in a confined narrow region along the boundary on the lower-potential side of Hall bars in the transition region of $2 < \nu$. The CE was concluded to arise from anomalous electron distribution comprising the electron accumulation in the higher $n = 1$ Landau level and the depletion in the lower $n = 0$ edge states.

This work is supported by Grant-in-Aid for Specially Promoted Research from the Japanese Ministry of Education, Culture, Sports, Science and Technology and by Solution Oriented Research for Science and Technology (SORST), Japan Science and Technology Corporation (JST).

[1] B. J. van Wees *et al.*, Phys. Rev. Lett. **62**, 1181 (1989).
[2] S. Komiyama *et al.*, Phys. Rev. B **40**, 12 566 (1989).
[3] B. J. van Wees *et al.*, Phys. Rev. B **39**, 8066 (1989).
[4] R. J. Haug and K. von Klitzing, Europhys. Lett. **10**, 489 (1989).
[5] P. L. McEuen *et al.*, Phys. Rev. Lett. **64**, 2062 (1990).
[6] S. Komiyama *et al.*, Solid State Commun. **80**, 157 (1991).
[7] P. C. van Son, F.W. de Vries, and T. M. Klapwijk, Phys. Rev. B **43**, 6764 (1991).
[8] V. T. Dolvopolov *et al.*, Solid State Commun. **78**, 999 (1991).
[9] S. Komiyama and H. Nii, Physica (Amsterdam) **184B**, 7 (1993).
[10] S. Komiyama *et al.*, Phys. Rev. B **45**, 11 085 (1992).
[11] R. Merz *et al.*, Phys. Rev. Lett. **70**, 651 (1993).
[12] A. Lorke *et al.*, Phys. Rev. B **53**, 1054 (1996).
[13] S. H. Tessmer *et al.*, Nature (London) **392**, 51 (1998); G. Finkelstein *et al.*, Science **289**, 90 (2000); N. B. Zhitenev *et al.*, Nature (London) **404**, 473 (2000).
[14] K. L. McCormick *et al.*, Phys. Rev. B **59**, 4654 (1999); Y. Kawano and T. Okamoto, Appl. Phys. Lett. **84**, 1111 (1994).
[15] Y. Kawano *et al.*, Phys. Rev. B **59**, 12 537 (1999).
[16] Y. Kawano and S. Komiyama, Phys. Rev. B **61**, 2931 (2000); **68**, 85328 (2003).
[17] K. Ikushima, H. Sakuma, and S. Komiyama, Rev. Sci. Instrum. **74**, 4209 (2003).
[18] Y. Kawano, Y. Hisanaga, H. Takenouchi, and S. Komiyama, J. Appl. Phys. **89**, 4037 (2001).
[19] A. Wurtz *et al.*, Phys. Rev. B **65**, 075303 (2002).
[20] The ratio B/B_D is adjusted to achieve maximum signals; typically, $B/B_D = 1.03$. The filling factor ν of the sample was controlled by tuning n_s of the sample; for instance, ν varies from 1.70 to 2.22 as n_s increases from 2.47×10^{15} m^{-2} to 3.22×10^{15} m^{-2} at $B = 6.0$ T. The n_s tuning, made via light-emitting diode illumination and backgate biasing, is necessary because the applicable range of B_D, where the detector sensitivity is sufficiently high, is narrow (5.9–6.2 T).
[21] The opposite two boundaries were not distinguished in Ref. [11].
[22] The presence of voltage probes is not clearly discerned in Figs. 2(a), 4(b), and 4(c). This is probably because the $n = 1$ LL is substantially reflected at the voltage probe arms with a relatively large aspect ratio (100 μm length and 40 μm width) and the unequal occupation between the LLs is substantially unaffected.
[23] Strictly, the obtained resonance curve is distorted because the filling factor varies from $\nu = 2.2$ to 2.5 over the B range of spectrum. The ν dependence of CE intensity (Fig. 5), however, makes it probable that the distortion is insignificant. The apparent resonance peak position ($B = 6.08$ T) corresponds to a cyclotron effective mass of $m_c^* = (0.0702 \pm 0.0007)m_0$. [Similar measurements for the hot spots derive $m_c^* = (0.0711 \pm 0.0007)m_0$.]
[24] CE is invisible in the interior region (Figs. 2 and 4). This indicates that generation of holes ($n = 0$ for $2 < \nu$) or electrons ($n = 1$ for $\nu < 2$) is not substantial in the interior region; viz., the effective electron temperature T_{eff} is not significantly different from the lattice temperature.
[25] H. Aoki, Appl. Phys. Lett. **48**, 559 (1986).